Integration of Deep Learning and Graph Theory for Analyzing Histopathology Whole-slide Images

Hyun Jung
Advanced Biomedical Computational Science
Frederick National Laboratory for Cancer Research sponsored by the National Cancer Institute
Frederick, MD, USA
hyun.jung@nih.gov

Elijah F. Edmondson
Laboratory Animal Sciences Program
Frederick National Laboratory for Cancer Research sponsored by the National Cancer Institute
Frederick, MD, USA
elijah.edmondson@nih.gov

Yanling Liu
Advanced Biomedical Computational Science
Frederick National Laboratory for Cancer Research sponsored by the National Cancer Institute
Frederick, MD, USA
liuy5@mail.nih.go

Christian Suloway
Advanced Biomedical Computational Science
Frederick National Laboratory for Cancer Research sponsored by the National Cancer Institute
Frederick, MD, USA
christian.suloway@nih.gov

David R. Morcock
AIDS and Cancer Virus Program
Frederick National Laboratory for Cancer Research sponsored by the National Cancer Institute
Frederick, MD, USA
morcockd@mail.nih.gov

Jack R. Collins
Advanced Biomedical Computational Science
Frederick National Laboratory for Cancer Research sponsored by the National Cancer Institute
Frederick, MD, USA
collinja@mail.nih.gov

Tianyi Miao
Advanced Biomedical Computational Science
Frederick National Laboratory for Cancer Research sponsored by the National Cancer Institute
Frederick, MD, USA
tianyi.miao@nih.gov

Claire Deleage
AIDS and Cancer Virus Program
Frederick National Laboratory for Cancer Research sponsored by the National Cancer Institute
Frederick, MD, USA
claire.deleage@nih.gov

Curtis Lisle
Knowledge Vis, LLC
Maitland, FL, USA
clisle@knowledgevis.com

***Abstract*—Characterization of collagen deposition in immunostained images is relevant to various pathological conditions, particularly in human immunodeficiency virus (HIV) infection. Accurate segmentation of these collagens and extracting representative features of underlying diseases are important steps to achieve quantitative diagnosis. While a first order statistic derived from the segmented collagens can be useful in representing pathological evolutions at different timepoints, it fails to capture morphological changes and spatial arrangements. In this work, we demonstrate a complete pipeline for extracting key histopathology features representing underlying disease progression from histopathology whole-slide images (WSIs) *via* integration of deep learning and graph theory. A convolutional neural network is trained and utilized for histopathological WSI segmentation. Parallel processing is applied to convert 100K ~ 150K segmented collagen fibrils into a single collective attributed relational graph, and graph theory is applied to extract topological and relational information from the collagenous framework. Results are in good agreement with the expected pathogenicity induced by collagen deposition, highlighting potentials in clinical applications for analyzing various meshwork-structures in whole-slide histology images.**

Keywords—histopathology, whole-slide image, deep learning, graph theory

I. Introduction

Histopathology studies signs of disease using the microscopic examination of a biopsy or surgical specimen. The sections are dyed with different stains to visualize different components of the tissue microscopically [1]. The underlying tissue architecture remains intact and it enables a comprehensive view of disease and its effect on tissues. As a result, the diagnosis from a histopathology image remains the "gold standard" in diagnosing a considerable number of diseases including almost all types of cancer [1].

Previously, a number of papers in the area of computational image analysis utilized "hand-crafted" algorithms for quantitative analysis of histopathology images. However, these traditional approaches have difficulties in accounting for all possible variances in morphology, texture, and color appearances. Thus, the "hand-crafted" approach might require substantial effort to capture a wide range of diversity [2]. Deep learning (DL), on the other hand, is a representation learning approach ideally suited to quantitative analysis tasks in histopathology images. Deep learning has had many successes in image classification challenges, as witnessed from AlexNet, VGGNet to ResNet [3]–[5], as well as biomedical image segmentation tasks [6], [7]. The main reason of unprecedented performance by deep learning is its capability of deriving high-level features that generalize well in a data-driven fashion.

Histopathology images have distinctive characteristics which set them apart from other images. These traits are high resolutions, complex appearances, diverse magnifications, various stains, and the corresponding differences in semantic interpretations [8]. Considering the diversity and complexity involved in interpreting such image data, one of the most promising methods for histopathology image analysis is the use of graph-based techniques. Graphs are flexible and effective tools receiving major interest for their expressive capability in modeling topological and relational information between image components [8]. Moreover, histopathological image data is visually observed and interpreted by pathologists by considering the morphological changes, neighborhood relationships, and spatial arrangements between tissue structures, which graphs have proven to be able to quantitatively represent [8]. However, graph-based methods are also frequently applied to regions of interest (ROIs) sampled from histopathology WSIs due to the limited computational resources and lack of advanced parallel

978-1-5386-9306-3/18/$31.00 ©2018 IEEE

processing techniques, limiting comprehensive views of the tissue structure, organization, and a deeper understanding of the underlying disease conditions, which are the main advantages of analyzing the WSIs [8].

In this work, we present a complete pipeline for analyzing network-forming collagens in histopathology WSIs *via* the integration of deep learning and graph theory techniques. Our contribution is in the integrated approach of the convolutional neural network (CNN) and graph-based methods to extract and analyze quantifiable features at the scale of whole tissue sections to correlate the underlying tissue responses with disease progression. Collagen deposition in histopathology images of lymph nodes in simian immunodeficiency virus (SIV) infected rhesus monkeys, which is particularly relevant to pathological conditions in HIV/SIV infection [9], is selected as the model to demonstrate the capabilities of our work.

II. Method

A. Image Pre-processing

Due to the typical ultrahigh resolution of histopathology images, original WSIs at 20× magnification are divided into smaller non-overlapping patches (400 × 400) for analysis. Thirty initial representative patches are chosen for generating ground truth labels using threshold and manual refinement. This initial ground truth labels are reviewed by pathologists and utilized for training a support vector machine (SVM) to generate an additional 1,798 ground truth labels. A total of 1,828 collagen patches and corresponding labels are augmented using rotation (− 90° and 90°), flip (vertical and horizontal), and random combinations of color variation. A total of 34,732 patches are prepared and 20,840 (60%) patches are used for the training, with the rest of the patches (13,892) being equally divided for the validation and testing sets.

U-Net has proven to be an effective CNN in biomedical image segmentation [6], [7]. U-Net is composed of contraction and expansion paths with skip-connections to enable pixel-wise segmentation of input images (Fig. 1). Our implementation utilizes 3 × 3 convolutions with reflective padding to keep the input and output image sizes the same. The rest of the network remains the same compared to the original implementation [6]. There are other CNN models focusing on segmenting medical images (DeepMedic [10], ScaleNet [11], *etc.*). However, in this work, we concentrated on demonstrating an integrated approach using deep learning and graph theory for analyzing network-forming collagens. Performance comparison between different CNN models for analyzing a collagenous network will be addressed in our future work. Dice coefficient loss (negative dice coefficient) is utilized as a loss function and minimized during the training. With the learning rate of 10^{-4}, the U-Net is trained for 40 epochs with batch size of 8. During the training, a model with the highest validation dice score is saved (0.9423) and it achieved 0.9444 dice score for the testing set. Segmentation patches created by the neural network are collected and stitched together to generate a segmentation mask of the input WSI.

III. Graph Theory

Each segmented collagen is converted into an undirected attributed relational graph (ARG) [12] by algorithms implemented in Python (Fig. 2(a)-(d)) [13]. Before the conversion, the segmentation mask is skeletonized and connected components are labeled using 8-connectivity [14]. After labeling the connected components (*i.e.* collagens), nodes and branches are assigned depending on the number of adjacent neighbors and converted into the ARGs [13]. A single WSI contains approximately 100K ~ 150K collagens. Their nodes, edges, and edge lengths (coded as edge weights in the graph structure) are saved in comma separated value (CSV) formatted files. Then the recorded values for each WSI are combined into slide-level undirected graph objects [15]. Individual graph objects are then created for each subset of connected components in the graph object of the whole slide image. Global features (*e.g.* diameter, radius, giant connected component ratio, *etc.*) [16] are computed for each connected component graph object, using parallelization in the Python multiprocessing module, and then aggregated for the whole slide image (Fig. 2(e)).

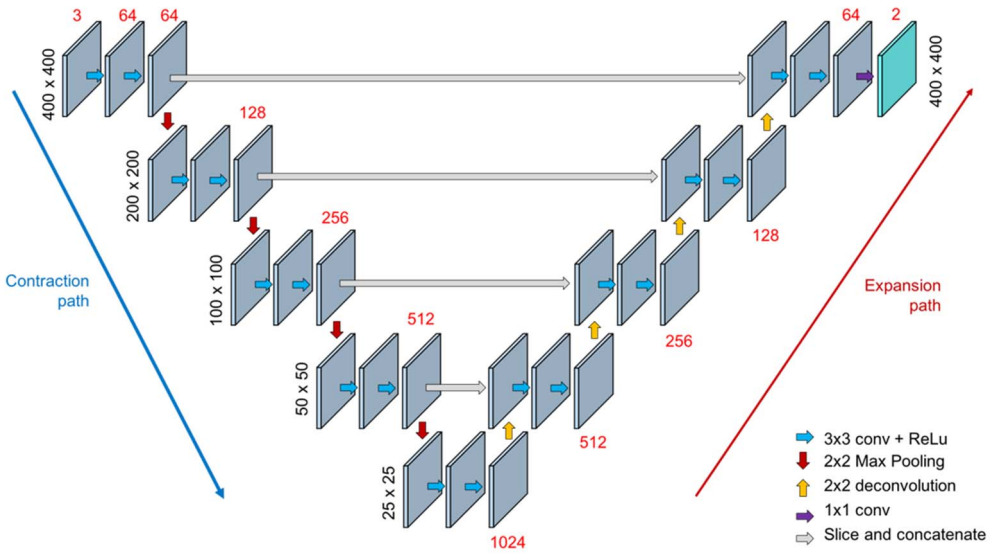

Fig. 1. Schematic diagrams of U-Net adapted from [6]. The sizes of input images and features maps are specified in black and red, respectively.

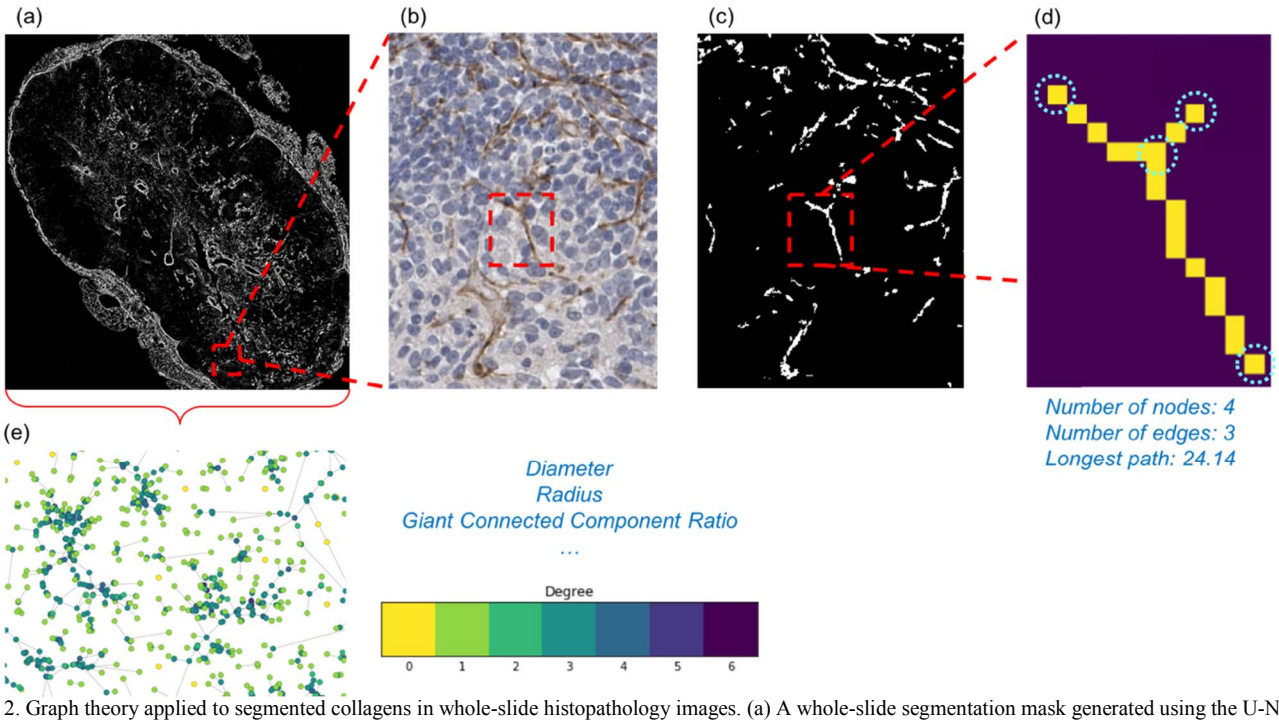

Fig. 2. Graph theory applied to segmented collagens in whole-slide histopathology images. (a) A whole-slide segmentation mask generated using the U-Net. (b, c) Enlarged view of the region of interest from the whole-slide histopathology image and corresponding segmentation mask. (d) Illustration of how a single collagen is converted into an undirected attributed relational graph with four nodes (highlighted in sky blue) and three edges (in yellow). (e) Small portion of an attributed relational graph containing every segmented collagen in the WSI. A circle and a line represent a single node and an edge in a collagen, respectively. Different colors represent the node's degree (number of edges). Global features (*e.g.* diameter, radius, and giant connected component ratio, *etc.*) are extracted from the graph.

IV. Results and Discussion

Histopathology WSIs of rhesus macaques at different timepoints (healthy, post infection of SIV, and after treatment using combination antiretroviral therapy (cART) with antifibrotic agent) have been analyzed using the pipeline proposed in this work. NCI-Frederick is accredited by AAALAC International and follows the Public Health Service Policy for the Care and Use of Laboratory Animals. Animal care was provided in accordance with the procedures outlined in the "Guide for Care and Use of Laboratory Animals" (National Research Council; 2011; National Academy Press; Washington, D.C.). One of the main advantages of processing WSIs as a whole is visualizing potential heterogeneity within anatomical sub-compartments of the lymph node. As shown in Fig. 3, a whole-slide histopathology of the lymph node (Fig. 3(a)) is processed using the trained U-Net. An enlarged view of the ROI is shown in Fig. 3(b) and the corresponding collagen segmentation mask generated is in Fig. 3(c). A collagen density heatmap is generated based on the ratio between the collagen positive pixels and the total number of pixels within a 50 × 50 pixel area (2,500 pixels). The follicles located in the medullary cords area in the SIV infected lymph node, which were manually identified and reviewed by pathologists, show lower collagen density compared to the surrounding compartments (Fig. 3(d)).

Quantification of a first order statistic (collagen density) as a feature for representing the underlying disease progression can be useful. As shown in Fig. 4(a), collagen densities are the highest in the medullary cords and T-Cell zone after the SIV infection except the follicle, which is consistent with the finding in Fig. 3(d). After treatment with the cART and antifibrotic agent, the collagen density decreased significantly in the medullary cords where the collagens are densely deposited, which corresponds to the expected disease progression. However, the collagen density alone is not capable of capturing the morphological evolutions and spatial arrangements of the collagen deposition in the lymph node.

On the other hand, global features (Fig. 4(b) and (c)) that are extracted using the collective ARGs reveal underlying changes of the collagen deposition. The diameter and radius (the maximum and minimum shortest path lengths from one node to any other node in the graph, respectively) increase after the SIV infection, indicating the elongation of the collagens. Both the diameter and radius need to be monitored simultaneously to ensure that the collagens are indeed elongated. Otherwise, one of the features (diameter/radius) can decrease/increase when the other parameter is increasing/decreasing. After the treatment, both the diameter and radius decrease while still remaining higher than the baseline (healthy tissue). On the other hand, the giant connected component ratio (GCCR, a ratio between the number of nodes in the largest connected component in the graph and total the number of nodes) shows a different trend compared to the previous features: a significant increase after the treatment. This observation indicates that the collagen with the largest number of nodes relatively remain the same, while the collagens with smaller number of nodes are treated more effectively resulting in a decrease in the overall total number of nodes. These results demonstrate the combined extraction of the global features using graph theoretical approaches enables quantitative representation of pathological evolutions at different timepoints and provides further insight into the structural changes of the collage deposition.

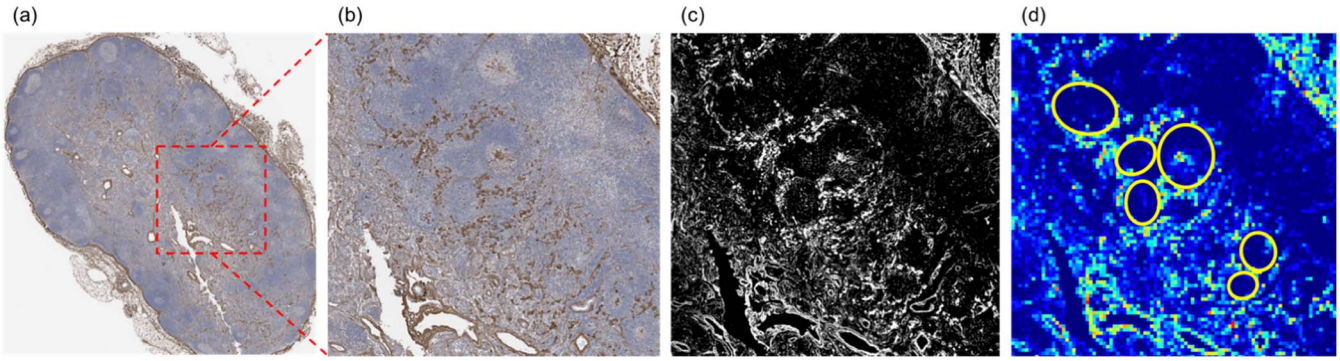

Fig. 3. (a) Lymph node whole-slide histopathology image of SIV infected rhesus macaques. Region of interest is highlighted in red dotted rectangle. (b) Enlarged view of the region of interest and (c) corresponding segmentation mask. (d) Heatmap generated using (c). Follicles located in the medullary cords area are highlighted in yellow circles.

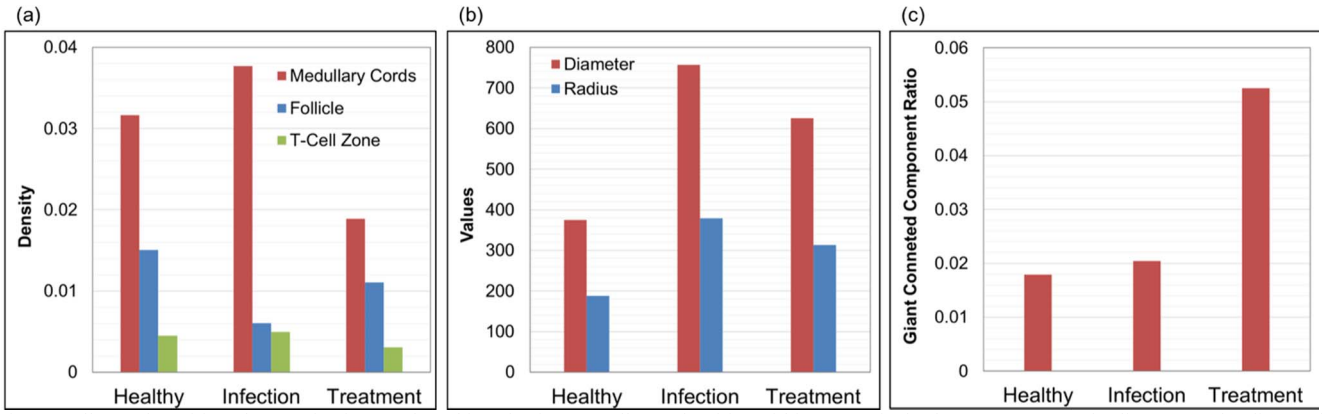

Fig. 4. Collagen deposition characterization results achieved using (a) collagen densities within anatomical sub-compartments, (b) diameter and radius, and (c) giant connected component ratio at different timepoints.

V. Conclusion

We have proposed an integrated approach that combines collagen segmentation generated by a CNN with graph theoretic post-processing. This enables extraction of quantifiable measures from immunohistochemistry stained WSIs to evaluate pathogenicity induced by collagen deposition at the scale of whole tissue sections.

The U-Net is trained and utilized to segment the collagen deposition in the histopathology images at different timepoints. The segmented collagens within the WSI are converted into a single collective ARG using parallel processing and then global features are extracted.

The global features show the clear advantage of capturing morphological evolutions of each collagen fiber and the spatial arrangements associated with the underlying pathological changes. Our future research will focus on extracting and contextualizing key quantifiable histopathology features representing underlying disease progression. We believe this will greatly facilitate the analysis of various meshwork-structures in histopathology whole-slide images in clinical applications. Also, extension of our proposed method into 3D volume and applying different CNN models should further increase the accuracy of estimating biological changes occurring in the tissue samples.

Acknowledgment

This project has been funded in whole or in part with Federal funds from the National Cancer Institute, National Institute of Health, under Contract No. HHSN261200800001E. The content of this publication does not necessarily reflect the views or policies of the Department of Health and Human Services, nor does mention of trade names, commercial products, or organizations imply endorsement by the U.S. Government.

References

[1] R. Rubin, D. S. Strayer, E. Rubin, and J. M. McDonald, Rubin's Pathology: Clinicopathologic Foundations of Medicine. Lippincott Williams & Wilkins, 2008.

[2] A. Janowczyk and A. Madabhushi, "Deep learning for digital pathology image analysis: A comprehensive tutorial with selected use cases," J. Pathol. Inform., vol. 7, no. 1, p. 29, 2016.

[3] A. Krizhevsky, I. Sutskever, and G. E. Hinton, "ImageNet Classification with Deep Convolutional Neural Networks," Adv. Neural Inf. Process. Syst., pp. 1–9, 2012.

[4] K. Simonyan and A. Zisserman, "Very Deep Convolutional Networks for Large-Scale Image Recognition," pp. 1–14, 2014.

[5] S. Wu, S. Zhong, and Y. Liu, "Deep residual learning for image steganalysis," Multimed. Tools Appl., pp. 1–17, 2017.

[6] O. Ronneberger, P. Fischer, and T. Brox, "U-Net: Convolutional Networks for Biomedical Image Segmentation," in Medical Image Computing and Computer-Assisted Intervention -- MICCAI 2015, 2015, pp. 234–241.

[7] H. Chen, X. Qi, L. Yu, Q. Dou, J. Qin, and P. A. Heng, "DCAN: Deep contour-aware networks for object instance segmentation from histology images," Med. Image Anal., vol. 36, pp. 135–146, 2017.

[8] H. Sharma, N. Zerbe, S. Lohmann, K. Kayser, O. Hellwich, and P. Hufnagl, "A review of graph-based methods for image analysis in digital histopathology," Diagn. Pathol., vol. 1, no. 1, pp. 1–51, 2015.

[9] J. D. Estes, A. T. Haase, and T. W. Schacker, “The role of collagen deposition in depleting CD4+ T cells and limiting reconstitution in HIV-1 and SIV infections through damage to the secondary lymphoid organ niche,” Semin. Immunol., vol. 20, no. 3, pp. 181–186, 2008.

[10] K. Kamnitsas et al., “Efficient multi-scale 3D CNN with fully connected CRF for accurate brain lesion segmentation,” Med. Image Anal., vol. 36, pp. 61–78, 2017.

[11] L. Fidon et al., “Scalable multimodal convolutional networks for brain tumour segmentation,” Lect. Notes Comput. Sci. (including Subser. Lect. Notes Artif. Intell. Lect. Notes Bioinformatics), vol. 10435 LNCS, pp. 285–293, 2017.

[12] A. Sanfeliu, A. Sanfeliu, and K. S. Fu, “A Distance Measure Between Attributed Relational Graphs for Pattern Recognition,” IEEE Trans. Syst. Man Cybern., vol. SMC-13, no. 3, pp. 353–362, 1983.

[13] E. W. Koch and E. W. Rosolowsky, “Filament identification through mathematical morphology,” Mon. Not. R. Astron. Soc., vol. 452, no. 4, pp. 3435–3450, 2015.

[14] R. C. Gonzalez and R. E. Woods, Digital Image Processing, 4th ed. Pearson, 2018.

[15] A. A. Hagberg, D. A. Schult, and P. J. Swart, “Exploring network structure, dynamics, and function using NetworkX,” Proc. 7th Python Sci. Conf. (SciPy 2008), no. SciPy, pp. 11–15, 2008.

[16] C. C. Bilgin, S. Ray, B. Baydil, W. P. Daley, M. Larsen, and B. Yener, “Multiscale feature analysis of salivary gland branching morphogenesis,” PLoS One, vol. 7, no. 3, 2012.